■ KNEE

ISTA Award 2023: Toward functional reconstruction of the pre-diseased state in total knee arthroplasty

P. Tzanetis,
R. Fluit,
K. de Souza,
S. Robertson,
B. Koopman,
N. Verdonschot

From University of Twente, Enschede, the Netherlands

Aims

The surgical target for optimal implant positioning in robotic-assisted total knee arthroplasty remains the subject of ongoing discussion. One of the proposed targets is to recreate the knee's functional behaviour as per its pre-diseased state. The aim of this study was to optimize implant positioning, starting from mechanical alignment (MA), toward restoring the pre-diseased status, including ligament strain and kinematic patterns, in a patient population.

Methods

We used an active appearance model-based approach to segment the preoperative CT of 21 osteoarthritic patients, which identified the osteophyte-free surfaces and estimated cartilage from the segmented bones; these geometries were used to construct patient-specific musculoskeletal models of the pre-diseased knee. Subsequently, implantations were simulated using the MA method, and a previously developed optimization technique was employed to find the optimal implant position that minimized the root mean square deviation between pre-diseased and postoperative ligament strains and kinematics.

Results

There were evident biomechanical differences between the simulated patient models, but also trends that appeared reproducible at the population level. Optimizing the implant position significantly reduced the maximum observed strain root mean square deviations within the cohort from 36.5% to below 5.3% for all but the anterolateral ligament; and concomitantly reduced the kinematic deviations from 3.8 mm (SD 1.7) and 4.7° (SD 1.9°) with MA to 2.7 mm (SD 1.4) and 3.7° (SD 1.9°) relative to the pre-diseased state. To achieve this, the femoral component consistently required translational adjustments in the anterior, lateral, and proximal directions, while the tibial component required a more posterior slope and varus rotation in most cases.

Conclusion

These findings confirm that MA-induced biomechanical alterations relative to the pre-diseased state can be reduced by optimizing the implant position, and may have implications to further advance pre-planning in robotic-assisted surgery in order to restore pre-diseased knee function.

Cite this article: ***Bone Joint J*** **2024;106-B(11):1231–1239.**

Introduction

Total knee arthroplasty (TKA) is a highly effective operation in treating end-stage knee osteoarthritis (OA), yet some patients report limited function of the implanted joint, impacting overall satisfaction after surgery.[1] Optimal positioning of the implant has been described as one of the determinants of postoperative functional outcomes,[2] and remains a subject of discussion.[3] Knee implants are traditionally placed according to mechanical alignment (MA) principles, striving to restore a neutral mechanical axis of the lower limb. This systematic approach, however, disregards the patient-specific, pre-diseased knee anatomy and may induce

Correspondence should be sent to P. Tzanetis; email: p.tzanetis@utwente.nl

doi:10.1302/0301-620X.106B11.BJJ-2023-1357.R1 $2.00

Bone Joint J 2024;106-B(11):1231–1239.

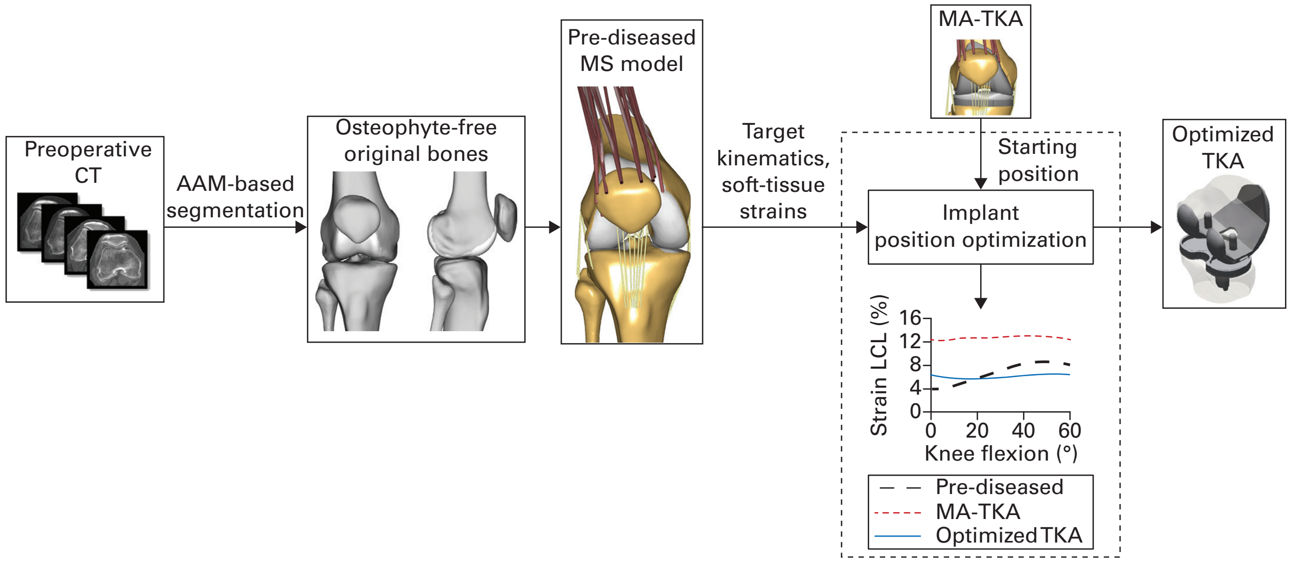

Fig. 1

Schematic of the study's workflow, including preoperative CT of the patient's lower limb, active appearance model (AAM)-based image segmentation, patient-specific musculoskeletal (MS) modelling of the pre-diseased and mechanically aligned (MA) knee, and MS model-based optimization, which finds the optimal implant position to recreate the pre-diseased knee biomechanical profiles. An example showcases the lateral collateral ligament (LCL) strain during flexion in the pre-diseased (black dashed curve), MA (red dash-dotted curve), and optimized (solid blue curve) total knee arthroplasty (TKA) models; the same comparison was performed for other ligaments and kinematic parameters. This flow required approximately one hour to process the segmented geometries and personalize the MS knee model, and 32 additional hours to find the optimal implant position for each patient, utilizing a 64-core 2.9 GHz processor.

non-physiological tension of the periarticular soft-tissues and, consequently, altered kinematics.[4]

Previous research suggests that restoring constitutional varus knees to neutral may be suboptimal, necessitating some degree of medial soft-tissue releases to achieve symmetrical, balanced flexion, and extension gaps;[5] the effects of over-correcting preoperative varus deformity have been shown in several studies.[6,7] It therefore appears necessary to define a more individualized positioning target based on the patient's knee phenotype.[8] Utilizing robotic-assisted TKA enables the pursuit of alternative alignment strategies, allowing for a personalized approach to implant positioning.[3]

Restoration of the pre-diseased functional status in a personalized manner can be defined as a logical target for robotic-assisted surgery. Recently, the functional alignment technique with a preoperative MA plan has been proposed to re-establish joint line obliquity of the knee as prior to the onset of the disease, subject to the mediolateral soft-tissue laxity profiles, while restoring pre-diseased knee kinematics.[9,10] Furthermore, the surgical precision with robotic assistance contributes to making these positioning targets more reproducible, with minimal postoperative outliers,[11] although the degree of improvement in functional outcomes appears inconsistent.[12-14] This implies that optimal implant position may vary based on the unique morphology of the patient's knee, and it is important to preoperatively simulate the biomechanical effects of implant positioning in order to ensure optimal postoperative joint function.

Previously, we have used active appearance modelling-based techniques to recreate the patient's knee morphology as it was before the appearance of osteophytes, referred to here as the pre-diseased state from a geometrical point of view. Based on this information, we constructed a personalized musculoskeletal model of the pre-diseased knee; following that, we developed a musculoskeletal model-driven optimization workflow, which considered a MA knee implant and, subsequently, optimized its position in order to mimic the pre-diseased knee's biomechanical behaviour over the flexion and extension range.[15]

The rationale of this workflow is to advance further the pre-planning in robotic-assisted surgery, while also being applicable to conventional TKA procedures performed without robotic assistance. This will be achieved by providing quantitative information, including detailed patient-specific ligament strains and tibiofemoral kinematics of the pre-diseased and implanted knee over the range of joint motion, which could aid surgeons in formulating an optimal, personalized preoperative plan. For this specific application, we chose MA as the initial plan, which is an established practice for the pre-planning software embedded within a commercially available robotic system. Nevertheless, the workflow remains adaptable to incorporate any other alignment philosophy.

The aim of this study was first to quantify deviations in ligament strains and consequent tibiofemoral kinematics, comparing mechanically implanted with their corresponding pre-diseased knees over a population of patients and, second, to utilize the pre-defined optimization technique, fine-tuning the implant position, in order to recreate the pre-diseased functional profiles of each patient as closely as possible. This study ultimately sought to establish how much we could gain by employing a personalized approach relative to MA, how large

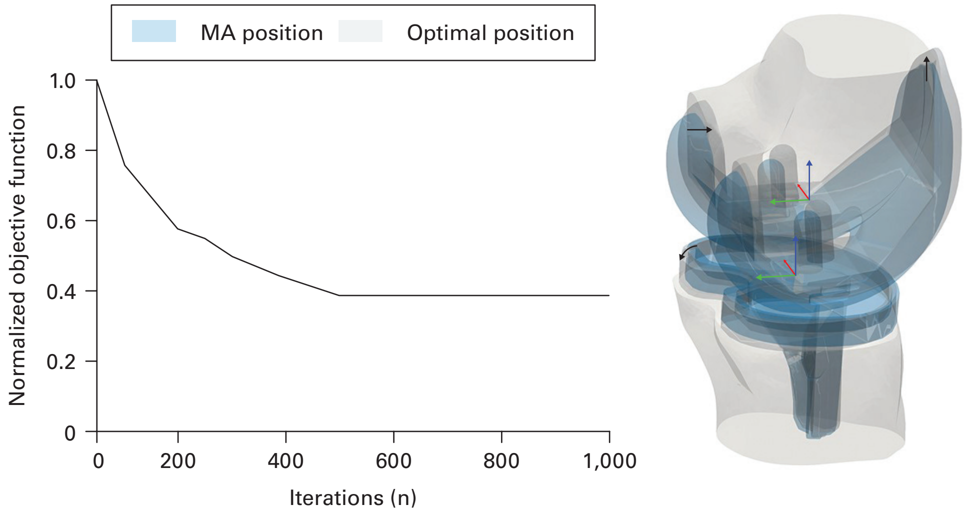

Fig. 2

a) The progression of the normalized objective function value over the number of iterations for a single, representative patient case, starting from the mechanical alignment (MA) position (value 1) and reaching the optimal implant position (approximate value 0.4), which corresponds to a 61.3% reduction. b) Illustration of the optimally positioned implant in situ relative to MA position for this particular case. Black arrows complement this visualization, highlighting certain positional adaptations of the components. The displayed coordinate systems represent the origin and orientation of the optimized femoral and tibial component position, respectively.

the component positional changes were with regard to MA, and whether these changes exhibited clear patterns.

Methods

The data used in this study were part of the knee functional flexion axis dataset.[16] Preoperative CT scans of bilateral lower limbs were collected from 21 OA patients, featuring different stages of osteophyte severity, who underwent primary TKA, performed using the Stryker Knee Navigation system (Stryker, USA). These images were automatically segmented using an active appearance model-based methodology to reconstruct the hip, ankle, and OA knee bone surfaces.[17] An osteophyte volume detection algorithm,[18] provided by Imorphics (Stryker, UK), was employed to subtract the osteophytic features from the outer surface of the cortical bone and recreate the osteophyte-free femoral and tibial bone geometries (pre-diseased state).[17,19,20] Related techniques have been validated elsewhere.[21] The articular cartilage of the pre-diseased knee was estimated by applying an MRI-derived training shape model that follows an established segmentation protocol.[22] Anatomical landmarks were extracted from the segmented hip, ankle, and pre-diseased knee bones to determine the origin and orientation of the femoral, tibial, and patellar reference frames based on a predefined convention.[23]

As described in an earlier study,[17] the generated knee structures reflecting the pre-diseased state, including bones and cartilage, of this cohort of patients were used to morph the geometry of a musculoskeletal reference model and to estimate the ligament attachment sites, applying a non-linear morphing technique;[24] these personalized models are described here as the pre-diseased knees from a geometrical perspective (Figure 1).

Strains of the anterior cruciate ligament (ACL), posterior cruciate ligament (PCL), deep medial collateral ligament (dMCL), superficial medial collateral ligament (sMCL), lateral collateral ligament (LCL), anterolateral ligament (ALL), oblique popliteal ligament (OPL), and posterior capsule (PC) were calculated for each patient, simulating a knee extension motion from 60° to 0° with only the gravitational force acting along the longitudinal axis of the system. Tibial kinematics relative to the femur, including anterior-posterior (AP), lateral-medial (LM), and proximal-distal (PD) translations, and external-internal (EI) and varus-valgus (VV) rotations, were estimated over the same arc of motion based on Grood and Suntay's definition.[25]

The patient-specific models were implanted with the Triathlon single-radius, cruciate-retaining total knee system (Stryker, USA) according to the principles of MA. The MA position was automatically determined using pre-planning software by Stryker, leveraging the patient's preoperative CT image, bone segmentations, and anatomical landmarks.

Sizing of the femoral component ensured anatomical congruence with the condyles, preventing anterior cortex notching greater than 3 mm, as this is associated with periprosthetic fracture,[26] and mediolateral overhang exceeding 3 mm, which may cause soft-tissue impingement and consequent postoperative pain.[27] Accordingly, the size selection of the tibial component ensured tibial coverage with minimal tray overhang at the cortical bone edges. The implants had a tibial insert thickness of 9 mm, which is a common choice in clinical practice and has been shown to offer a good compromise between the depth of tibial resection and strains of the collateral ligaments.[28,29] Surgeons could opt for an alternative available insert thickness, depending on the intraoperative stability assessment. The patellae were not resurfaced. The MA-TKA models simulated the same activity as the pre-diseased models to study the effect of mechanical implantation on the ligament strains and kinematics.

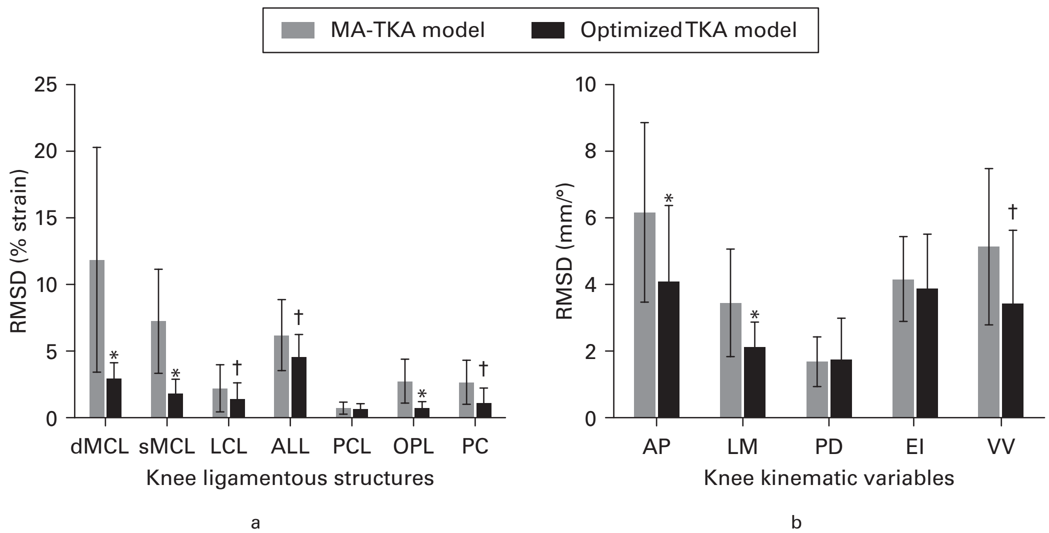

Fig. 3

Root mean square deviation (RMSD) in the a) strain of the ligamentous structures and b) tibiofemoral kinematic variables between pre-diseased and total knee arthroplasty (TKA) models with mechanical alignment (MA) and optimized implant position. The bars show the mean values, while the whiskers indicate the SD. ALL, anterolateral ligament; AP, anterior-posterior; dMCL, deep medial collateral ligament; EI, external-internal; LCL, lateral collateral ligament; LM, lateral-medial; PC, posterior capsule; PCL, posterior cruciate ligament; PD, proximal-distal; OPL, oblique popliteal ligament; sMCL, superficial medial collateral ligament; VV, varus-valgus.*p < 0.01, †p < 0.05.

Differences in the predicted strain and kinematic curves between the pre-diseased and MA-TKA models were quantified using the root mean square deviation (RMSD). An optimization algorithm that we developed in previous work was subsequently used to find the optimal position of the components that minimized the RMSD between the pre-diseased and postoperative biomechanical profiles.[15] The objective function of this optimization problem consisted of three distinct components: the first two, equally weighted components involved the summation of the RMSD for each individual ligament strain and kinematic variable, respectively, while the third pertained to a penalty factor added to the resulting function value, as provided in the following equation:

$$\min_{x \in \mathbb{R}^n} \left(\left(\sum_{i=1}^{m_{str}} w_{str_i} \sqrt{\frac{1}{t} \sum_{\theta=0}^{\theta_{end}} (y_{imp\_str_{i,\theta}}(x) - y_{pre\_str_{i,\theta}})^2} \right) + \left(\sum_{j=1}^{m_{kin}} w_{kin_j} \sqrt{\frac{1}{t} \sum_{\theta=0}^{\theta_{end}} (y_{imp\_kin_{j,\theta}}(x) - y_{pre\_kin_{j,\theta}})^2} \right) + P \right) \tag{1}$$

$$lb < x < ub$$

where x indicates the degrees of freedom of the components subject to the lower and upper bounds, denoted as lb and ub, respectively; the boundary conditions were defined relative to MA. More precisely, the translational variation of the femoral component was constrained to within approximately 6 mm in the AP, LM, and PD directions, whereas the translational placement of the tibial component was maintained unchanged to ensure convergence to a global optimum position. The rotational variation of the femoral and tibial components was confined within approximately 3° and 6°, respectively, for flexion-extension (FE), and within approximately 6° for EI and VV rotations. Further, n indicates the dimension of the solution space equal to the number of x positional variables ($n = 9$), m is the number of strain or kinematic variables involved in the objective function, and w is the weighting factor assigned to the i^{th} ligament and j^{th} kinematic variable, which was calculated such that the strain and kinematic errors were given equal importance. Finally, t denotes the number of discrete time steps of the model simulation ($t = 60$) from 0° to 60° (θ_{end}), and y indicates the predicted strain or kinematic value of the i^{th} ligament and j^{th} kinematic variable, respectively, for the x positional variable in the implanted model configuration, or in the pre-diseased situation, at flexion angle θ.

A penalty factor, denoted as P and set equal to 10^3 – the objective function's output was in the order of magnitude 10^2 – was applied to the objective function if the force residual at any given flexion angle, as calculated by the model's force-dependent kinematics solver,[30] exceeded the specified tolerance of 5 N, thus ensuring dynamic consistency of the simulations. In case multiple positioning solutions resulted in similar objective function values, indicating minimal deviations relative to the pre-diseased state, the solutions closest to MA were chosen to facilitate their clinical feasibility.[31] Figure 1 provides a schematic description of the study's workflow spanning preoperative image segmentation to musculoskeletal modelling and model-based implant positioning optimization. To assess the effect of optimization on minimizing the strain and kinematic deviations between the pre-diseased and MA-TKA models, we used the non-parametric Wilcoxon signed-rank test, and set the significance level to $p < 0.05$.

Results

Large variations in the pre-diseased ligament strain and tibiofemoral kinematic profiles were observed among the 21 patient cases. The standardized MA could not accommodate

Table I. Implant positional adjustments required to recreate the pre-diseased functional conditions with reference to mechanical alignment. Positive values denote posterior, medial, and proximal translations, and flexion, internal, and varus rotations.

Patient	Femoral component						Tibial component*		
	Translation, mm			Rotation, °			Rotation, °		
	AP	LM	PD	FE	EI	VV	FE	EI	VV
1	-2.9	-1.9	1.8	0.1	-4.9	1.9	3.7	2.9	5.7
2	-0.2	-1.9	3.0	0.8	-2.2	1.8	4.1	-0.8	2.7
3	-0.5	-0.9	4.4	0.9	-4.0	-0.3	1.6	-1.0	1.8
4	-1.8	-5.5	0.4	0.1	-2.0	0.5	1.2	1.9	4.1
5	-1.7	-2.5	1.5	0.5	-5.2	2.2	5.1	-1.8	0.0
6	-3.3	-2.9	0.7	-0.2	1.5	-0.9	0.8	1.0	3.8
7	-1.7	-2.3	3.3	-1.1	-3.3	4.2	4.2	0.3	0.5
8	0.1	-3.0	2.8	-0.4	-1.3	1.6	3.6	-0.1	4.0
9	-3.6	-2.4	2.5	-1.0	-1.3	-0.5	3.7	-1.6	2.1
10	-2.0	-2.1	0.1	-0.6	-1.9	-2.5	3.1	0.7	2.2
11	-4.1	-3.4	2.4	0.3	0.9	1.2	4.4	1.9	0.2
12	-2.8	-0.5	2.0	-0.2	-1.1	0.1	3.0	-1.0	2.1
13	-0.1	-0.7	0.4	-0.2	-3.2	0.9	4.6	-2.3	3.5
14	-3.5	-1.3	2.3	-0.8	-0.9	-0.7	3.1	-1.2	1.6
15	-3.2	-1.3	0.3	-0.3	1.3	-2.0	2.6	-1.6	3.4
16	-2.3	-2.5	3.1	-0.1	-3.7	1.5	2.8	-0.2	2.2
17	-2.8	-3.0	4.4	0.2	0.3	-3.5	2.6	-0.8	1.5
18	-4.3	-4.2	1.2	0.6	-3.2	0.6	0.5	-2.7	0.9
19	-2.3	-1.0	0.9	0.6	0.3	1.3	4.7	1.0	0.6
20	-1.3	-0.3	2.3	0.7	-0.6	-2.5	1.6	-0.7	-0.7
21	-1.5	-4.7	5.4	1.7	1.6	-2.9	-2.6	-2.0	3.1
Range†	-4.3 to 0.1	-5.5 to -0.3	0.3 to 5.4	-1.1 to 1.7	-5.2 to 1.6	-3.5 to 4.2	-2.6 to 5.1	-2.7 to 2.9	-0.7 to 5.7

*The translational position of the tibial component in all three directions remained unchanged.
†Including the endpoints.
AP, anterior-posterior; EI, external-internal; FE, flexion-extension; LM, lateral-medial; MA, mechanical alignment; PD, proximal-distal; VV, varus-valgus.

these individual profiles. Consequently, adopting a personalized, targeted approach became necessary to achieve optimal implant positioning. Strains of the ligaments in the MA-TKA models exhibited deviations of up to 36.5% in the medial collateral ligaments (dMCL (3.0 to 36.5), sMCL (1.7 to 17.7)), 6.2% and 13.8% in the lateral collateral (LCL, 0.0 to 6.2) and anterolateral (ALL, 2.2 to 13.8) ligaments, respectively, and up to 7.5% in the posterior ligamentous structures (PCL (0.1 to 1.8), OPL (0.2 to 7.5), PC (0.4 to 7.2)) relative to the pre-diseased state. The predicted knee kinematics showed a RMSD of 3.8 mm (SD 1.7) for translations and 4.7° (SD 1.9°) for rotations compared to their corresponding pre-diseased knee over all patients. The optimization process resulted, on average, in a 48.6% reduction of the objective function value compared to the MA position among patients. Figure 2 depicts the progression of the objective function value for an individual, representative patient case, starting from the MA position and reaching the optimal position. For all patients, optimizing the implant position reduced the strain deviations to less than 5.3% in the dMCL (1.2 to 5.3) and sMCL (0.3 to 4.1), 4.1% and 8.5% in the LCL (0.0 to 4.1) and ALL (2.1 to 8.5), respectively, and 3.7% in the PCL (0.1 to 1.8), OPL (0.2 to 2.0), and PC (0.2 to 3.7) structures in relation to the pre-diseased state; and resulted in kinematic deviations of 2.7 mm (SD 1.4) and 3.7° (SD 1.9°). Intra-patient comparison revealed significantly lower deviations in the AP and LM translations and VV rotation with the optimized TKA models compared to MA controls. Similarly, the reduction in ligament strains was significant for all ligaments except for the PCL (Figure 3). The required adjustments in the position of the femoral and tibial components to reproduce the biomechanical status of the pre-diseased knees are summarized in Table I.

Discussion

This study investigated the effect of mechanically and optimally aligning a knee implant, aiming to reproduce physiological ligament strains and tibiofemoral kinematics across a patient population. To achieve this, we compared MA-TKA models with their pre-diseased counterparts, and subsequently used a formerly established technique to optimize the implant position, thereby recreating the pre-diseased knee functional status as closely as feasibly possible. The findings of this study suggest that adjusting the position of the individual components relative to MA results in a closer match between the pre-diseased and postoperative biomechanical conditions. We found variable optimal positions among patients, but could identify distinct positional patterns within the patient population that enabled us to achieve the surgical target.

MA of the knee implant had a clinically important effect on the strains of the ligaments, with concomitant changes in the tibiofemoral kinematics. The dMCL and sMCL strains were consistently larger in the MA-TKA models, exhibiting mean deviations of 11.9% and 7.3%, respectively, compared to the pre-diseased state among patients (Figure 3). This corroborates the work of Delport et al,[32] who showed that restoration to absolute neutral MA can increase the collateral strain deviations from the native knee during passive flexion-extension.

Provenzano et al[33] identified the onset of fibre plastic deformation at 5.1% strain in the medial collateral ligamentous structures; sub-failure strains above the specified threshold can induce nearly complete ligament disruption and, postoperatively, increased medial laxity, hindering the overall functional stability. The observed higher strains in the medial collaterals in our study could conceptually be associated with the relatively large valgus angulation, as reflected in the VV results (Figure 3). Although the LCL showed a relatively low average strain deviation at 2.2% from the pre-diseased knee, individual deviations, such as those observed in one patient case (6.2%), cannot be disregarded and may cause pain when exceeding the ultimate ligament strain.[34]

The ALL reported clinically relevant strain deviations at a mean of 6.2%, which could be due to larger anterior tibial translation during flexion.[35] Such deviations may have consecutively contributed to the increased EI rotational deviations, as this ligament restricts internal tibial rotation,[36] although the functional role of the ALL is still controversial.[37]

Optimizing the implant position resulted in a statistically significant reduction in the average strain deviations of the medial (< 3.0%) and lateral (1.4%) collateral ligaments and posterior capsular structures (< 1.1%) (Figure 3) within the clinically acceptable range.[32,33,38] These results are consistent with other research that emulated native collateral ligament elongation patterns using a patient-specific, model-driven response surface methodological technique.[39]

Although, statistically, there was a significant reduction of the ALL strain deviation at 4.7% on average from the pre-diseased knee, some individual patient models exhibited deviations of up to 8.5%, well above the pre-defined damage threshold,[33] which are likely to be related to the nearly unchanged EI angulation and could lead to anterolateral knee pain. Modifying the objective function to give more weight to the strain of the particular ligament could potentially mitigate this issue.

Following the ligament adjustments, there was a concomitant reduction of the observed mean kinematic deviations by 28.9% for translations and 21.2% for rotations, resulting in a RMSD of 2.7 mm and 3.7°, respectively (Figure 3). This aligns with a recent study,[40] which approximated native kinematics within a similar order of deviations based on cadaveric model-based artificial neural network optimization.

The AP translational deviations in our study remained higher than in the pre-diseased situation for some patients; in one case, the disparity in the overall AP displacement of the tibia relative to the femur reached up to 9.3 mm, which may be in part due to the altered geometry and conformity of the articular surface. Patient-specific implants have been shown to reduce such deviations, exhibiting femoral rollback closer to the normal knee than standard designs since they better match the shape of the patient's knee.[41,42]

The optimal position of the implant was found to be within 4 mm and 4° from MA in 70% of patients, which is a clinically acceptable range from the MA position of the components,[43-45] although some patients required slightly larger changes. This implies that MA is a reasonable functional target that can be improved utilizing techniques similar to the one proposed in this study.

The precise positional adjustments revealed certain directional pathways toward achieving optimal placement of the individual components. In most patient cases, the femoral component was placed in a more anterior, lateral, and proximal position, rotated externally relative to the tibia, with increasing varus alignment of the tibial component. Placing the femoral component in a more proximal position could lead to the elevation of the joint line, which is not desired.[46] This suggests that the initial femoral component position was comparatively at a lower level relative to the pre-diseased knee; nevertheless, whether this originates from assumptions inherent in the pre-diseased model or the MA procedure remains to be determined.

Coronal alignment of the femoral component was more variable and less clear, but the majority of patients still required some degree of varus. Bellemans et al[5] described that a relevant proportion of the normal knees has a limb alignment of 3° varus or more; therefore, slight under-correction to approximate pre-diseased alignment, as might have occurred in our study, could be more physiological for these patients,[47] potentially producing functional results close to the pre-diseased situation.

Although some patients required internal rotation of the femoral component, more than half exhibited an externally rotated component. External rotation within 5° (Table I) using the central referencing technique seems acceptable, with minimal compromise of the mediolateral condylar symmetry.[48,49] The surgeons should, however, be aware of component overhanging that could arise at the posterior aspect of the lateral condyle, which can cause impingement with the capsular fibres. Further, it is important to consider that excessively rotating the femoral component either internally or externally has consequences for patellar tracking,[50] potentially inducing anterior knee pain.[51]

At the tibial level, Innocenti et al[52] showed that repositioning the tibial component to 2° and up to 6° varus intuitively increased the strain in the LCL beyond physiological capacity, as compared to neutral mechanical configuration, which could detrimentally affect clinical outcomes. These findings, however, were not confirmed in the current study, possibly because the concurrent rotational adjustment of the femoral component compensated for any such effect. Furthermore, the tibial component consistently required more posterior slope in the optimal position relative to MA. This is in agreement with an earlier investigation, which suggested that increasing the tibial slope with reference to the centre of the tibial plateau is relevant to restoring the biomechanics of the native knee.[53] Surgeons often strive for a slope between 0° and 7° based on the implant manufacturer's recommendations; the average slope in the present study was 3.1° (SD 1.3°), falling inside this range. Nonetheless, it is important to consider individual variations in native tibial slopes, as insufficient slope correction may inhibit the overall stability of the joint.[54]

The strength of this simulation-based study is that it thoroughly examines the feasibility of postoperatively restoring the pre-diseased knee function in a population of OA patients, which would be unfeasible in a cadaveric or intraoperative setting. Furthermore, it attempts to quantify the knee ligament strains and kinematics as they were before the onset of the disease in a patient-specific biomechanical situation and, subsequently, to use this information to optimize the position of the implant with regard to the existing MA technique.

It is important to emphasize, however, that we do not intend to replace the existing alignment philosophies, but rather to present a framework for recreating the knee's pre-diseased biomechanical conditions. This could help guide the formulation of a personalized preoperative plan, feeding a robotic system with that specified target for its precise execution. Intraoperatively, the surgeon may further adjust the component's position, if necessary, until the desired symmetry in the mediolateral gaps is achieved, following the functional alignment principles. With our rationale, the laxities would be expected to approximate closely those of the pre-diseased state. Our methodology can additionally aid in selecting different TKA designs or designing a more personalized implant which better matches the patient's pre-diseased articular geometry, employing the osteophyte-free active appearance model-based technique, which maintains alignment results close to normal kinematics.

The present study has some limitations. First, the accuracy of the model predictions has not been assessed against experimental measurements of soft-tissue strains and knee kinematics. Previous validation of comparable models revealed kinematic errors in the order of observed deviations,[24,55] which accentuates the relevance of performing dynamic, in vivo measurements of knee mechanics in response to implant position to determine the accuracy and reliability of the model outputs before the patient-specific clinical application.

Second, the menisci were excluded from the pre-diseased knee models since these were not distinct structures to segment from the CT scans. This may have caused tibiofemoral kinematic alterations, for instance in the posterior and mediolateral displacement, as well as internal rotation, of the tibia relative to the femur,[56] potentially resulting in a disparity between the actual kinematic behaviour of a pre-diseased knee and the model's predictions.

Third, the ligament mechanical properties were not patient-specific but instead derived from comparable intact knee models in the literature and remained unmodified in the implanted configuration, although they are likely to change over time due to OA. Nonetheless, using the same ligament properties for both pre-diseased and implanted models ensured equal levels of uncertainty in their predictions, which eventually allowed us to isolate the influence of implantation on the joint's mechanics. Further analysis could involve incorporating intraoperative laxity information, acquired possibly through the software of a robotic total knee system, into the musculoskeletal model; this would allow refinement of the ligament mechanics, thereby simulating the inherent laxities existing in OA patients.

Fourth, the models were limited to simulating only a gravity-assisted flexion-extension activity; in theory, it would be possible to analyze other motor tasks, as previously reported,[29] yet the particular activity can be performed intraoperatively to assess whether the joint is adequately aligned and whether the surrounding soft-tissues are appropriately tensioned to allow for a balanced motion during flexion and extension. Another fact worth discussing is that this study focused solely on the MA technique. Employing alternative alignment techniques, such as the (restricted) kinematic alignment, may alter the deviations observed between the implanted and pre-diseased knee models, consequently impacting the positional adjustments required toward reproducing the pre-diseased biomechanical situation.

In particular, kinematic alignment has been used to re-establish the obliquity and level of the femoral and tibial joint lines to the native knee.[57] This could theoretically result in kinematics that more closely resemble those of the pre-diseased. Nevertheless, our model-based approach advances these considerations further by enabling a detailed quantification of the soft-tissue strains and kinematics across the flexion and extension range, which is unfeasible to monitor preoperatively irrespective of the alignment technique employed.

We should further acknowledge that the recreation of the pre-diseased state depends on the patient's Coronal Plane Alignment of the Knee (CPAK) type,[58] which was not considered in this study. Classifying the patients into their respective CPAK type would possibly help identify in advance those patients who would benefit most from a personalized alignment approach over systematic MA or any other alignment philosophy. This could provide more insight into the adaptations required in the implant's position for each patient and the observed positioning trends.

Two aspects deserve emphasis in this context: firstly, our focus was specifically on the intra-knee alignment of the joint, excluding an analysis of the overall limb alignment, or relevant parameters such as the hip-knee-ankle angle, which is integral to the CPAK classification; secondly, and most importantly, patients in the current study were categorized according to their own individual phenotype – the pre-diseased functioning of their knee. Furthermore, the study results may have been influenced by the use of a standard, single-radius, cruciate-retaining implant design, and hence they should be interpreted within the context of this choice.

Recent evidence suggests that alternative designs, such as the medial-pivot or bicruciate-retaining prostheses, have a direct influence on postoperative knee biomechanics;[59,60] therefore, testing other implant designs would help determine whether the observed deviations and positioning trends persist or are largely affected by design. Finally, given that the proposed method lacks clinical validation, a clinical trial is necessary to assess whether it aids in improving the postoperative functional outcomes and, ultimately, patient satisfaction.

In conclusion, MA-TKA can induce clinically relevant changes in the strains of the ligaments and tibiofemoral kinematics compared to the knee's pre-diseased condition, which could, be mitigated by optimizing the position of the components. Optimal placement was variable and patient-specific, yet certain trajectories in the spatial positioning of the femoral and/or tibial components were identified at the population level for the implant design studied. These findings provide relevant information to quantify the positional target in robotic-assisted TKA toward reconstructing the pre-diseased functional state of the knee as closely as possible, thereby improving knee function and overall patient satisfaction.

Take home message

- Mechanical alignment in total knee arthroplasty may induce clinically relevant alterations in ligament strains and knee kinematics compared to the knee's pre-diseased state. These biomechanical alterations could be mitigated by optimizing the position of the components.
- The implant's optimal position was variable and patient-specific, yet certain positional trajectories were identified at the population level for a cruciate-retaining design.
- This methodology can assist the formulation of a personalized plan for implant positioning that can be executed precisely through robotic-assisted surgery.

Social media

Follow P. Tzanetis on X @TzanetisP

References

1. **Bourne RB**, **Chesworth BM**, **Davis AM**, **Mahomed NN**, **Charron KDJ**. Patient satisfaction after total knee arthroplasty: who is satisfied and who is not? *Clin Orthop Relat Res*. 2010;468(1):57–63.
2. **Rivière C**, **Iranpour F**, **Auvinet E**, **et al**. Alignment options for total knee arthroplasty: a systematic review. *Orthop Traumatol: Surg Res*. 2017;103(7):1047–1056.
3. **Oussedik S**, **Abdel MP**, **Victor J**, **Pagnano MW**, **Haddad FS**. Alignment in total knee arthroplasty. *Bone Joint J*. 2020;102-B(3):276–279.
4. **Rivière C**, **Iranpour F**, **Auvinet E**, **et al**. Mechanical alignment technique for TKA: are there intrinsic technical limitations? *Orthop Traumatol Surg Res*. 2017;103(7):1057–1067.
5. **Bellemans J**, **Colyn W**, **Vandenneucker H**, **Victor J**. The Chitranjan Ranawat award: is neutral mechanical alignment normal for all patients? The concept of constitutional varus. *Clin Orthop Relat Res*. 2012;470(1):45–53.
6. **Anijs T**, **Wolfson D**, **Verdonschot N**, **Janssen D**. Population-based effect of total knee arthroplasty alignment on simulated tibial bone remodeling. *J Mech Behav Biomed Mater*. 2020;111:104014.
7. **Vanlommel L**, **Vanlommel J**, **Claes S**, **Bellemans J**. Slight undercorrection following total knee arthroplasty results in superior clinical outcomes in varus knees. *Knee Surg Sports Traumatol Arthrosc*. 2013;21(10):2325–2330.
8. **Slevin O**, **Hirschmann A**, **Schiapparelli FF**, **Amsler F**, **Huegli RW**, **Hirschmann MT**. Neutral alignment leads to higher knee society scores after total knee arthroplasty in preoperatively non-varus patients: a prospective clinical study using 3D-CT. *Knee Surg Sports Traumatol Arthrosc*. 2018;26(6):1602–1609.
9. **Kayani B**, **Konan S**, **Tahmassebi J**, **Oussedik S**, **Moriarty PD**, **Haddad FS**. A prospective double-blinded randomised control trial comparing robotic arm-assisted functionally aligned total knee arthroplasty versus robotic arm-assisted mechanically aligned total knee arthroplasty. *Trials*. 2020;21(1):194.
10. **Clark G**, **Steer R**, **Wood D**. Functional alignment achieves a more balanced total knee arthroplasty than either mechanical alignment or kinematic alignment prior to soft tissue releases. *Knee Surg Sports Traumatol Arthrosc*. 2023;31(4):1420–1426.
11. **Hampp EL**, **Chughtai M**, **Scholl LY**, **et al**. Robotic-arm assisted total knee arthroplasty demonstrated greater accuracy and precision to plan compared with manual techniques. *J Knee Surg*. 2019;32(3):239–250.
12. **Ollivier M**, **Parratte S**, **Lino L**, **Flecher X**, **Pesenti S**, **Argenson J-N**. No benefit of computer-assisted TKA: 10-year results of a prospective randomized study. *Clin Orthop Relat Res*. 2018;476(1):126–134.
13. **Winnock de Grave P**, **Kellens J**, **Tampere T**, **Vermue H**, **Luyckx T**, **Claeys K**. Clinical outcomes in TKA are enhanced by both robotic assistance and patient specific alignment: a comparative trial in 120 patients. *Arch Orthop Trauma Surg*. 2023;143(6):3391–3399.
14. **Agarwal N**, **To K**, **McDonnell S**, **Khan W**. Clinical and radiological outcomes in robotic-assisted total knee arthroplasty: a systematic review and meta-analysis. *J Arthroplasty*. 2020;35(11):3393–3409.
15. **Tzanetis P**, **Fluit R**, **de Souza K**, **Robertson S**, **Koopman B**, **Verdonschot N**. Pre-planning the surgical target for optimal implant positioning in robotic-assisted total knee arthroplasty. *Bioengineering (Basel)*. 2023;10(5):543.
16. **Oussedik S**, **Scholes C**, **Ferguson D**, **Roe J**, **Parker D**. Is femoral component rotation in a TKA reliably guided by the functional flexion axis? *Clin Orthop Relat Res*. 2012;470(11):3227–3232.
17. **Tzanetis P**, **de Souza K**, **Robertson S**, **Fluit R**, **Koopman B**, **Verdonschot N**. Numerical study of osteophyte effects on preoperative knee functionality in patients undergoing total knee arthroplasty. *J Orthop Res*. 2024;42(9):1943–1954.
18. **Vincent G**, **Wolstenholme C**, **Scott I**, **Bowes M**. Fully automatic segmentation of the knee joint using active appearance models. **In**: *Medical Image Analysis for the Clinic: A Grand Challenge*. Vol 1. 2010: 224–230.
19. **Motesharei A**, **Batailler C**, **De Massari D**, **Vincent G**, **Chen AF**, **Lustig S**. Predicting robotic-assisted total knee arthroplasty operating time: benefits of machine-learning and 3D patient-specific data. *Bone Jt Open*. 2022;3(5):383–389.
20. **Bowes MA**, **Kacena K**, **Alabas OA**, **et al**. Machine-learning, MRI bone shape and important clinical outcomes in osteoarthritis: data from the Osteoarthritis Initiative. *Ann Rheum Dis*. 2021;80(4):502–508.
21. **Morton AM**, **Akhbari B**, **Moore DC**, **Crisco JJ**. Osteophyte volume calculation using dissimilarity-excluding Procrustes registration of archived bone models from healthy volunteers. *J Orthop Res*. 2020;38(6):1307–1315.
22. **Hunter DJ**, **Bowes MA**, **Eaton CB**, **et al**. Can cartilage loss be detected in knee osteoarthritis (OA) patients with 3–6 months' observation using advanced image analysis of 3T MRI? *Osteoarthr Cartilage*. 2010;18(5):677–683.
23. **Carbone V**, **Fluit R**, **Pellikaan P**, **et al**. TLEM 2.0 - a comprehensive musculoskeletal geometry dataset for subject-specific modeling of lower extremity. *J Biomech*. 2015;48(5):734–741.
24. **Marra MA**, **Vanheule V**, **Fluit R**, **et al**. A subject-specific musculoskeletal modeling framework to predict in vivo mechanics of total knee arthroplasty. *J Biomech Eng*. 2015;137(2):020904.
25. **Grood ES**, **Suntay WJ**. A joint coordinate system for the clinical description of three-dimensional motions: application to the knee. *J Biomech Eng*. 1983;105(2): 136–144.
26. **Zalzal P**, **Backstein D**, **Gross AE**, **Papini M**. Notching of the anterior femoral cortex during total knee arthroplasty. *J Arthroplasty*. 2006;21(5):737–743.
27. **Mahoney OM**, **Kinsey T**. Overhang of the femoral component in total knee arthroplasty: risk factors and clinical consequences. *J Bone Joint Surg Am*. 2010;92-A(5):1115–1121.
28. **Rajamäki A**, **Niemeläinen M**, **Junnila M**, **et al**. Thicker polyethylene inserts (≥ 13mm) increase the risk for early failure after primary cruciate-retaining total knee arthroplasty (TKA): a single-centre study of 7643 TKAs. *Knee Surg Sports Traumatol Arthrosc*. 2023;31(3):1018–1025.
29. **Tzanetis P**, **Marra MA**, **Fluit R**, **Koopman B**, **Verdonschot N**. Biomechanical consequences of tibial insert thickness after total knee arthroplasty: a musculoskeletal simulation study. *Appl Sci (Basel)*. 2021;11(5):2423.
30. **Skipper Andersen M**, **de Zee M**, **Damsgaard M**, **Nolte D**, **Rasmussen J**. Introduction to force-dependent kinematics: theory and application to mandible modeling. *J Biomech Eng*. 2017;139(9):091001.
31. **Schelker BL**, **Nowakowski AM**, **Hirschmann MT**. What is the "safe zone" for transition of coronal alignment from systematic to a more personalised one in total knee arthroplasty? A systematic review. *Knee Surg Sports Traumatol Arthrosc*. 2022;30(2):419–427.
32. **Delport H**, **Labey L**, **Innocenti B**, **De Corte R**, **Vander Sloten J**, **Bellemans J**. Restoration of constitutional alignment in TKA leads to more physiological strains in the collateral ligaments. *Knee Surg Sports Traumatol Arthrosc*. 2015;23(8): 2159–2169.
33. **Provenzano PP**, **Heisey D**, **Hayashi K**, **Lakes R**, **Vanderby R Jr**. Subfailure damage in ligament: a structural and cellular evaluation. *J Appl Physiol (1985)*. 2002;92(1):362–371.
34. **Smeets K**, **Slane J**, **Scheys L**, **Claes S**, **Bellemans J**. Mechanical analysis of extra-articular knee ligaments. Part One: native knee ligaments. *Knee*. 2017;24(5):949–956.
35. **Vincent J-P**, **Magnussen RA**, **Gezmez F**, **et al**. The anterolateral ligament of the human knee: an anatomic and histologic study. *Knee Surg Sports Traumatol Arthrosc*. 2012;20(1):147–152.
36. **Parsons EM**, **Gee AO**, **Spiekerman C**, **Cavanagh PR**. The biomechanical function of the anterolateral ligament of the knee. *Am J Sports Med*. 2015;43(3):669–674.
37. **Noyes FR**, **Huser LE**, **Levy MS**. Rotational knee instability in ACL-deficient knees: role of the anterolateral ligament and iliotibial band as defined by tibiofemoral compartment translations and rotations. *J Bone Joint Surg Am*. 2017;99-A: 305–314.
38. **Guo Z**, **Freeman JW**, **Barrett JG**, **De Vita R**. Quantification of strain induced damage in medial collateral ligaments. *J Biomech Eng*. 2015;137(7):071011.
39. **Quilez MP**, **Delport HP**, **Wirix-Speetjens R**, **et al**. Can standard implants reproduce the native kinematics of a TKA patient? 19th Annual Meeting of the International Society for Computer Assisted Orthopaedic Surgery (CAOS). 2019;3:311–314.
40. **Dejtiar DL**, **Bartsoen L**, **Wesseling M**, **et al**. Standard cruciate-retaining total knee arthroplasty implants can reproduce native kinematics. 19th Annual Meeting of the International Society for Computer Assisted Orthopaedic Surgery (CAOS). 2020;4:61–64.

41. **Patil S**, **Bunn A**, **Bugbee WD**, **Colwell CW Jr**, **D'Lima DD**. Patient-specific implants with custom cutting blocks better approximate natural knee kinematics than standard TKA without custom cutting blocks. *Knee*. 2015;22(6):624–629.
42. **Koh YG**, **Park KM**, **Kang KT**. The biomechanical effect of tibiofemoral conformity design for patient-specific cruciate retainging total knee arthroplasty using computational simulation. *J Exp Orthop*. 2019;6(1):23.
43. **Parratte S**, **Pagnano MW**, **Trousdale RT**, **Berry DJ**. Effect of postoperative mechanical axis alignment on the fifteen-year survival of modern, cemented total knee replacements. *J Bone Joint Surg Am*. 2010;92-A(12):2143–2149.
44. **Bonner TJ**, **Eardley WGP**, **Patterson P**, **Gregg PJ**. The effect of post-operative mechanical axis alignment on the survival of primary total knee replacements after a follow-up of 15 years. *J Bone Joint Surg Br*. 2011;93-B(9):1217–1222.
45. **Abdel MP**, **Ollivier M**, **Parratte S**, **Trousdale RT**, **Berry DJ**, **Pagnano MW**. Effect of postoperative mechanical axis alignment on survival and functional outcomes of modern total knee arthroplasties with cement: a concise follow-up at 20 years. *J Bone Joint Surg Am*. 2018;100-A(6):472–478.
46. **Luyckx T**, **Vandenneucker H**, **Ing LS**, **Vereecke E**, **Ing AV**, **Victor J**. Raising the joint line in TKA is associated with mid-flexion laxity: a study in cadaver knees. *Clin Orthop Relat Res*. 2018;476(3):601–611.
47. **Victor J**. Optimising position and stability in total knee arthroplasty. *EFORT Open Rev*. 2017;2(5):215–220.
48. **Slevin O**, **Moser LB**, **Hirschmann MT**. Is there an optimal TKA component position? In: *Basics in Primary Knee Arthroplasty*. Switzerland: Springer, Cham, 2022: 299–309.
49. **Bonnin MP**, **Saffarini M**, **Nover L**, **et al**. External rotation of the femoral component increases asymmetry of the posterior condyles. *Bone Joint J*. 2017;99-B(7): 894–903.
50. **Verlinden C**, **Uvin P**, **Labey L**, **Luyckx JP**, **Bellemans J**, **Vandenneucker H**. The influence of malrotation of the femoral component in total knee replacement on the mechanics of patellofemoral contact during gait: an in vitro biomechanical study. *J Bone Joint Surg Br*. 2010;92-B(5):737–742.
51. **Bell SW**, **Young P**, **Drury C**, **et al**. Component rotational alignment in unexplained painful primary total knee arthroplasty. *Knee*. 2014;21(1):272–277.
52. **Innocenti B**, **Bellemans J**, **Catani F**. Deviations from optimal alignment in TKA: is there a biomechanical difference between femoral or tibial component alignment? *J Arthroplasty*. 2016;31(1):295–301.
53. **Marra MA**, **Strzelczak M**, **Heesterbeek PJC**, **et al**. Anterior referencing of tibial slope in total knee arthroplasty considerably influences knee kinematics: a musculoskeletal simulation study. *Knee Surg Sports Traumatol Arthrosc*. 2018;26(5):1540–1548.
54. **Okazaki K**, **Tashiro Y**, **Mizu-uchi H**, **Hamai S**, **Doi T**, **Iwamoto Y**. Influence of the posterior tibial slope on the flexion gap in total knee arthroplasty. *Knee*. 2014;21(4):806–809.
55. **Vanheule V**, **Delport HP**, **Andersen MS**, **et al**. Evaluation of predicted knee function for component malrotation in total knee arthroplasty. *Med Eng Phys*. 2017;40:56–64.
56. **Hu J**, **Xin H**, **Chen Z**, **Zhang Q**, **Peng Y**, **Jin Z**. The role of menisci in knee contact mechanics and secondary kinematics during human walking. *Clin Biomech (Bristol, Avon)*. 2019;61:58–63.
57. **Lee YS**, **Howell SM**, **Won Y-Y**, **et al**. Kinematic alignment is a possible alternative to mechanical alignment in total knee arthroplasty. *Knee Surg Sports Traumatol Arthrosc*. 2017;25(11):3467–3479.
58. **MacDessi SJ**, **Griffiths-Jones W**, **Harris IA**, **Bellemans J**, **Chen DB**. Coronal Plane Alignment of the Knee (CPAK) classification. *Bone Joint J*. 2021;103-B(2):329–337.
59. **Putame G**, **Terzini M**, **Rivera F**, **Kebbach M**, **Bader R**, **Bignardi C**. Kinematics and kinetics comparison of ultra-congruent versus medial-pivot designs for total knee arthroplasty by multibody analysis. *Sci Rep*. 2022;12(1):3052.
60. **Arnout N**, **Victor J**, **Vermue H**, **Pringels L**, **Bellemans J**, **Verstraete MA**. Knee joint laxity is restored in a bi-cruciate retaining TKA-design. *Knee Surg Sports Traumatol Arthrosc*. 2020;28(9):2863–2871.

Author information:
P. Tzanetis, PhD, Postdoctoral Researcher of Orthopaedics and Musculoskeletal Biomechanics
B. Koopman, PhD, Professor of Biomechanical Engineering
Department of Biomechanical Engineering, University of Twente, Enschede, The Netherlands.

R. Fluit, PhD, Lecturer of Biomedical Engineering, Faculty of Science and Engineering, University of Groningen, Groningen, The Netherlands.

K. de Souza, PhD, Senior Manager of Clinical Intelligence
S. Robertson, MSc, Senior Engineer of AI Research
Stryker, Manchester, UK.

N. Verdonschot, PhD, Professor of Implant Biomechanics, Head of Orthopaedic Research Laboratory, Department of Biomechanical Engineering, University of Twente, Enschede, The Netherlands; Orthopaedic Research Laboratory, Radboud Institute for Health Sciences, Radboud University Medical Center, Nijmegen, The Netherlands.

Author contributions:
P. Tzanetis: Conceptualization, Data curation, Formal analysis, Investigation, Methodology, Software, Validation, Visualization, Writing – original draft, Writing – review & editing.
R. Fluit: Conceptualization, Methodology, Software.
K. de Souza: Data curation, Resources.
S. Robertson: Data curation.
B. Koopman: Project administration, Supervision.
N. Verdonschot: Conceptualization, Funding acquisition, Methodology, Project administration, Supervision, Writing – review & editing.

Funding statement:
The authors disclose receipt of the following financial or material support for the research, authorship, and/or publication of this article: this research was funded by Stryker European Operations Ltd., Ireland.

ICMJE COI statement:
This research was funded by Stryker European Operations Ltd., Ireland. P. Tzanetis, R. Fluit, and B. Koopman declare that they have no competing interests. K. de Souza is an employee of Stryker, and holds stock and stock options in Stryker Corporation. S. Robertson is also an employee of Stryker. N. Verdonschot is a consultant at Invibio Ltd. and Exactech.

Data sharing:
The datasets generated and analyzed in the current study are not publicly available due to data protection regulations. Access to data is limited to the researchers who have obtained permission for data processing. Further inquiries can be made to the corresponding author.

Acknowledgements:
P. Tzanetis was awarded the Early Career Investigator award by the International Society for Technology in Arthroplasty (ISTA) in 2023. The authors would like to acknowledge Eric Garling (Stryker, Amsterdam, The Netherlands), José-Luis Moctezuma (Stryker, Freiburg, Germany), and Daniele De Massari (Stryker, Amsterdam, The Netherlands) for their help in the acquisition of imaging data used in this study.

Ethical review statement:
The dataset provided by Stryker was fully anonymized, with all patients having provided informed consent for research purposes. Therefore, an IRB review was not required.

Open access funding:
The open access fee for this article was funded by Stryker.

This article was primary edited by A. Wood.